Journal of Materials Chemistry B

Accepted Manuscript

ROYAL SOCIETY OF CHEMISTRY

www.rsc.org/materialsB

Polyacryloyl Hydrazide Based Injectable & Stimuli Responsive Hydrogels with Tunable Properties

Anuj Kumar[†], *Sabindra K. Samal*[‡], *Rupesh Dash*[‡] *& Umaprasana Ojha**[,†]

[†]Department of Chemistry, Rajiv Gandhi Institute of Petroleum Technology Raebareli, Ratapur Chowk, UP-229316, India

[‡]Institute of Life Science, Bhubaneswar, Odisha, India

Abstract

Synthesis and characterization of a series of injectable and stimuli responsive hydrogels based on polyacryloyl hydrazide has been accomplished using dimethyl 2,2'-thiodiacetate, acrylic acid (AA), diethyl malonate and polyethylene glycol (PEGDA) as the cross-linkers through chemical or dual cross-linking pathway. The cross-linking reactions were carried out at room temperature or 70 °C to synthesize uniform and transparent gels. The swelling ratios ≈ 10–800% of the hydrogels depended on the type and concentration of the cross-linker, temperature and pH of the medium. A suitable combination of chemical and physical cross-linking was necessary to achieve optimum storage modulus of the gels. The yield stress of the gels synthesized using cross-linker concentrations up to 0.7 mol/L was

observed above 10% strain and the viscosity decreased by at least two orders of magnitude upon increasing the shear rate by 1000 times suggesting the gels may be smoothly injected through the needle. The gels released up to 10–84% of the total encapsulated Rhodamine B in a controlled manner over a period of 120 h under physiological conditions. The gels prepared using cross-linker concentrations up to 1.3 mol/L exhibited excellent water retention capacity (>95%) up to 40 days. Samples synthesized using AA and PEGDA as the cross-linker exhibited excellent cytocompatibility and are potential candidates for controlled delivery as well as non-evasive biomedical applications.

Introduction

Polymeric hydrogels owing to their softness, porosity, high water content, biocompatibility and mechanical integrity in aqueous medium have attracted a great deal of interest as candidates for therapeutic drug delivery[1], tissue engineering[2], patterning[3], microfluidics[4] aerogel[5] and enhanced oil recovery.[6,7] For example, photodegradable hydrogels were reported for possible modulation of cellular environments.[8] Hydrogels were designed to engineer neural stem cells used for regeneration of nervous system.[9]

Hydrogels those respond to various external stimuli such as pH, temperature and mechanical force have emerged as smart drug delivery materials.[10,11] For example, polypropylene phosphate based hydrogel gradually released 100% Lysozyme in 22 h.[12] Among various parameters, type and extent of cross-linking played an important role in determining the nature and effectiveness of release.[13,14] Both physical and chemical cross-linking procedures were important to prepare hydrogels for controlled release.[15,16] The presence of chemical cross-links provided stability and structural integrity in stringent environments, whereas the presence of transient or non-covalent cross-links such as hydrogen bonding, hydrophobic association and ionic interaction imparted toughness by dissipating

energy through facile dissociation and reformation of bonds.[17] These labile physical cross-links helped further by enhancing responsiveness of the gels to various external stimulai and broadened their applicability as self-healing and drug delivery materials.[18] The presence of reversible along with permanent cross-links also facilitated smooth injection of gels via shear thinning mechanism.[19] The initial modulus was retrieved on releasing shear stress due to reformation of the reversible cross-links. For example, Hebraud and coworkers have recently demonstrated the injectability of a dual cross-linked polyvinyl alcohol based hydrogels.[20] Therefore, use of dual cross-linking motif has emerged as an ideal way to prepare stable, injectable and stimulai responsive hydrogels.[21,22] However, a limited number of dual cross-linked hydrogels have been reported in literature so far.

Polyacryloyl hydrazide (PAH) readily dissolved in water under all pH conditions and the carbonyl hydrazide pendant functionality promptly reacted with a range of functional groups including, carboxylates, aldehydes, acrylates, epoxides and carboxylic acids under mild conditions.[23] A range of biocompatible hydrogels employing carbonyl hydrazide functionality as key cross-linking moiety have been developed and studied for different biomedical applications.[24,25] For example, Michael-type addition and Schiff's-base reactions were used in the past to synthesize in-situ biocompatible hydrogels implementing carbonyl hydrazide functional dextran and hyaluronans as precursors.[26,27] Therefore, PAH offered the possibility of developing a range of new dual cross-linked hydrogels using carboxylate, acrylate, sulfate, anhydride, aldehyde and carboxylic acid as cross-linkers. Recently we have reported an efficient and cost effective procedure to synthesize PAH from polymethyl acrylate (PMA) with quantitative functional group conversion.[23] An example of a pH responsive hydrogel using dimethyl 2,2'-thiodiacetate (DTDA) as cross-linker was also reported that showed controlled release ability of dye molecules under physiological conditions.

In this report, we have described the synthesis of a series of hydrogels using PAH as the precursor and DTDA, diethyl malonate (DEM), acrylic acid (AA), polyethylene glycol diacrylate (PEGDA) as cross-linkers. The gelation kinetics, swelling ratios and effect of external stimulai were studied with respect to PAH and cross-linker amount. Mechanical properties of the hydrogels were investigated and injectability of the gels was evaluated using rheological analysis. The dye release rate of all the hydrogels was determined under physiological conditions and cytocompatibility of the gels was studied.

Experimental

Materials. Methyl acrylate (s-d fine chem., >99%), potassium bromate (Merck, >99.0%), sodium hydrogen sulfite (Merck, 58.5–67.4%), sodium chloride (NaCl, Qualigens, >99.9%), hydrazine hydrate (s-d fine chem., 99%), tetra-n-butyl ammonium bromide (TBAB, Merck, ≥98.0%), thiodiglycolic acid (Acros Organics, 98.0%), sulfuric acid (Merck, 98%), ethyl acetate (Merck, ≥99.5%), sodium bicarbonate (Merck, ≥99.0%), acrylic acid (Merck, ≥99.0%), diethyl malonate (s-d fine chem., >98%), poly (ethylene glycol) diacrylate (Sigma Aldrich, ≤100%), potassium hydrogen phthalate (KHP, s-d fine chem., >99%), potassium dihydrogen phosphate (KH_2PO_4, Rankem, ≥99%), sodium hydrogen phosphate (Na_2HPO_4, SRL, >99%), borax anhydrous ($Na_2B_4O_7$, Sigma Aldrich, ≥98%), hydrochloric acid (HCl, s-d fine chem., 35–38%), potassium chloride (KCl, Himedia, 9.5%), 3-(4, 5-dimethylthiazol-2-yl)-2, 5-diphenyltetrazolium bromide (MTT, Sigma Alrich, ≥98.0%), ethidium bromide solution (EB, 10 mg/mL, Sigma Aldrich), acridine orange (AO, Sigma Aldrich, ≥95.0%), dulbecco's modified eagle's medium (DMEM, Sigma Aldrich, ≥99.9%), sodium dodecyl sulfate (SDS, Sigma Aldrich, ≥99.0%), 0.25% trypsin-0.1% ethylene diamine tetra acetate (EDTA) solution (Sigma Aldrich), 10% fetal bovine serum (Life Technology), 1% of penicillin-streptomycin (Life Technology), 96 well plates (BD biosciences, 353072) and

Rhodamine B (Lobachemie, >95.0%) were used as received. DTDA was synthesized from thiodiglycolic acid using a reported procedure.[28] Tetrahydrofuran (THF, s-d fine chem., >99.5%) was refluxed over sodium metal and benzophenone overnight and distilled under nitrogen atmosphere prior to use. In a typical purification procedure, the aqueous solution of PAH was added to methanol and kept undisturbed until the entire precipitate settled down. The same procedure was repeated with the precipitate three times. Finally the precipitate was dried in rotary evaporator under reduced pressure condition.

Instrumentation: The Perkin Elmer Spectrum Two FT-IR spectrometer was used to record FT-IR spectra of the samples as either solid or thin film. All samples were recorded using "Attenuated Total Reflectance" (ATR) mode. The PIKE MIRacle^{TM} single reflection horizontal ATR accessory equipped with ZnSe ATR crystal was used for recording the spectra. The hydrogels or thin films were gently pressed against the ATR crystal to record the spectra. Lab India UV–Vis 3200 was used to record UV–Vis Spectra of the sample. All the data were recorded at ~25 °C. The tensile studies were performed according to ASTM D638 using a H25K-S UTM Tinius Olsen extensometer. The samples were recorded as rectangular strips at ~25 °C using 25 kN load cell at a crosshead speed of 10 mm/min. The data represented here is an average of three specimens. Mechanical properties of the hydrogels were investigated by rheology. The rheological measurements were performed using Anton Paar Modular Compact Rheometer 302 (MCR 302) equipped with a sand-blasted plate−plate geometry to prevent slippage. All measurements were performed under Oscillatory mode at 25 °C unless otherwise noted. TC-10^{TM} automated cell counter purchased from Bio-Rad with optimal working conditions in the temperature range of 25–35 °C was used for counting the cells. 10 μL of cell suspension was taken in the TC-10 disposable counting slide with the help

of a 10 µL pipette. The slide was inserted into the counter and reading was taken within 5 min. Varioskan™ Flash Multimode Reader from Thermo Scientific equipped with a xenon flash light source was used for quantification of absorbance. Leica DM IL LED inverted microscope with integrated modulation contrast (IMC) and incident-light fluorescence mechanism was used to acquire photographs. The illumination was generated via EBQ 100-04 Hg 100 W lamp.

Synthesis of PAH: PAH was synthesized using a procedure reported by us previously.[23] A solution of PMA (M_n = 64000 gm/mol, PDI = 1.6, 15 gm, 0.234 mmol) in 450 mL of THF was placed in a one liter round-bottom flask. To it, hydrazine hydrate (58.2 gm, 1.15 mol) and TBAB (15 gm, 46.53 mmol) was added. The mixture was stirred at 60 °C for 12 h. The reaction mixture was cooled to room temperature and kept undisturbed till the layers separated out. The aqueous layer was transferred into methanol to precipitate the product polymer. The obtained white product was further washed with methanol several times to remove low molecular weight impurities and dried under vacuum at ambient temperature. Yield: 96%, ^{1}H NMR (500 MHz, D_2O): 1.2-2.3 (m, 3H, —C***H*****$_2$**—C***H***—CO—), 3.17 (br, 2H, —CONH—N***H*****$_2$**), FT-IR (thin film, cm^{-1}): 983 (m, C—N), 1445 (m, C—H), 1612 (s, C=O), 2925 (m, C—H), 3260 (m, N—H).

Synthesis of hydrogels

A series of PAH based hydrogels were synthesized using DTDA, AA, PEGDA and DEM as cross-linkers as shown in **Scheme 1**.

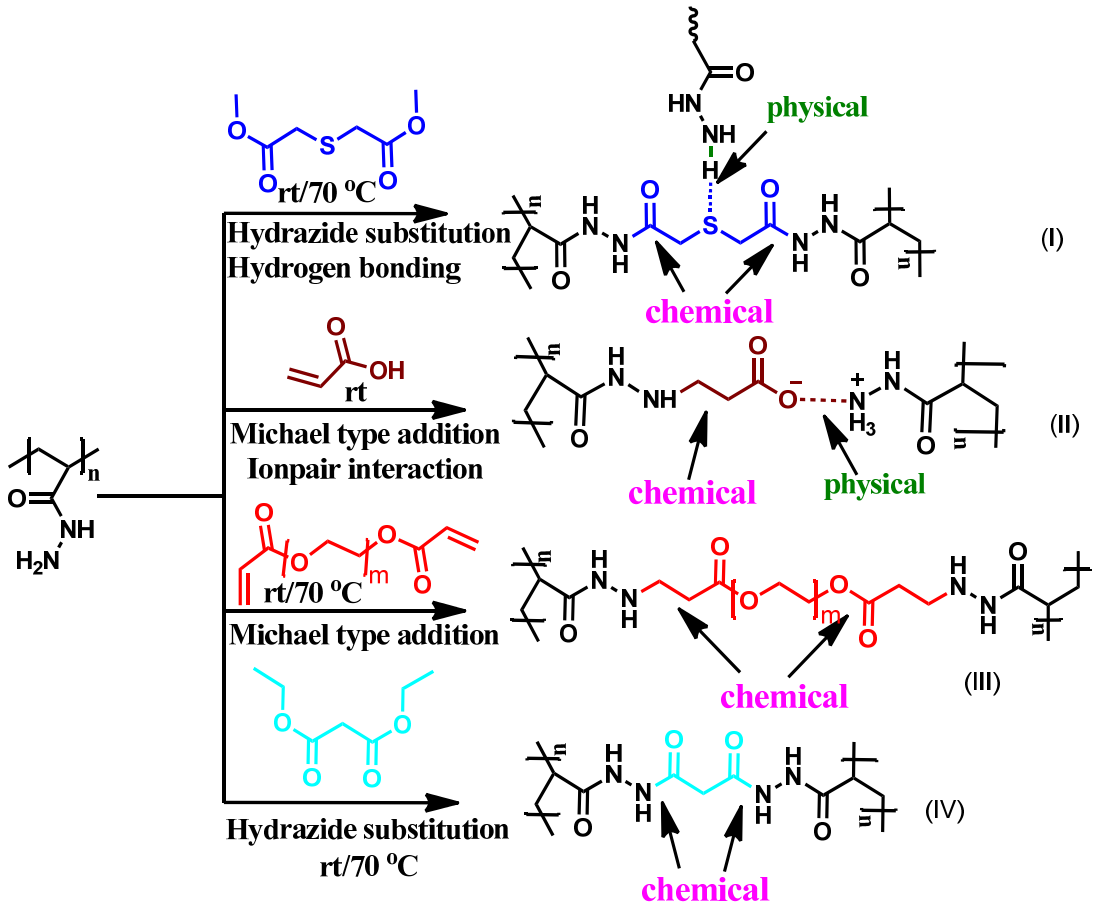

Scheme 1: General Synthetic scheme for PAH based hydrogels (I) (PAH-DTDA), (II) (PAH-AA), (III) (PAH-PEGDA), and (IV) (PAH-DEM).

PAH and DTDA based hydrogels (PAH-DTDA) (I): To 3.0 mL aqueous solution of PAH (0.6 gm, 9.4 µmol), DTDA (0.4 gm, 2.2 mmol, 0.7 mol/L) was added and the mixture was gently stirred in vertex mixture. The resulting solution was kept at room temperature undisturbed for 30 min to remove trapped air bubbles. Then the temperature of solution was raised to 70 °C. After 11 h, the uniform and transparent hydrogel formed was cooled to room temperature for further utilization. In a similar manner, a set of hydrogels were prepared by changing the amount of DTDA (0.7 gm, 3.9 mmol, 1.3 mol/L or 1.0 gm, 5.6 mmol, 1.9 mol/L) and PAH (0.9 gm, 14 µmol or 1.2 gm, 19 µmol) in solution. FT-IR (thin film, cm^{-1}):

662 (m, C—S), 1001 (s, N—N), 1331 (m, C—H), 1532 (m, C=O), 1643 (s, C=O), 2925 (m, C—H), 3260 (m, N—H).

PAH and AA based hydrogels (PAH-AA) (II): To 3.0 mL aqueous solution of PAH (0.6 gm, 9.4 μmol), AA (0.2 gm, 2.2 mmol, 0.7 mol/L) was added and the mixture was gently stirred in vertex mixture. The resulting solution was kept at room temperature undisturbed for 6 h to form the uniform and transparent hydrogels. In a similar manner, a set of hydrogels were prepared by changing the amount of AA (0.3 gm, 3.9 mmol, 1.3 mol/L or 0.4 gm, 5.6 mmol, 1.9 mol/L) and PAH (0.9 gm, 14 μmol or 1.2 gm, 19 μmol) in solution. FT-IR (thin film, cm^{-1}): 1113 (m, N—N), 1389 (s, C—H), 1551 (s, C=O), 1653 (m, C=O), 2925 (m, C—H), 3198 (m, N—H).

PAH and PEGDA based hydrogels (PAH-PEGDA) (III): To 3.0 mL aqueous solution of PAH (0.6 gm, 9.4 μmol), PEGDA (M_n = 258 gm/mol, 0.2 gm, 0.6 mmol, 0.2 mol/L) was added and the mixture was gently stirred in vertex mixture. The resulting solution was kept at room temperature undisturbed for 30 min to remove trapped air bubbles. Then the temperature of solution was raised to 70 °C. After 14 h, the uniform and transparent hydrogel formed was cooled to room temperature for further utilization. In a similar manner, a set of hydrogels were prepared by changing the amount of PEGDA (0.3 gm, 1.1 mmol, 0.4 mol/L or 0.6 gm, 2.2 mmol, 0.7 mol/L) and PAH (0.9 gm, 14 μmol or 1.2 gm, 19 μmol) in solution. FT-IR (thin film, cm^{-1}): 1063 (s, N—N), 1115 (m, C—O), 1450 (m, C—H), 1538 (m, C=O), 1647 (s, C=O), 2924 (m, C—H), 3264 (m, N—H).

PAH and DEM based hydrogels (PAH-DEM) (IV): To 3.0 mL aqueous solution of PAH (0.6 gm, 9.4 μmol), DEM (0.4 gm, 2.2 mmol, 0.7 mol/L) was added and the mixture was gently stirred in vertex mixture. The resulting solution was kept at room temperature undisturbed for 30 min to remove trapped air bubbles. Then the temperature of the solution was raised to 70 °C. After 10 h, the uniform and transparent hydrogel formed was cooled to

room temperature for further utilization. In a similar manner, a set of hydrogels were prepared by changing the amount of DEM (0.6 gm, 3.9 mmol, 1.3 mol/L or 0.9 gm, 5.6 mmol, 1.9 mol/L) and PAH (0.9 gm, 14 μmol or 1.2 gm, 19 μmol) in solution. FT-IR (thin film, cm^{-1}): 1036 (s, N—N), 1339 (s, C—H), 1532 (m, C=O), 1605 (s, C=O), 3046 (m, C—H), 3273 (m, N—H).

Swelling ratio measurement of the hydrogels synthesized using different amounts of PAH and cross linkers: The hydrogels were prepared as described above. Swelling ratios of the hydrogels were determined using gravimetric procedure. As-prepared gels were soaked in fixed amount of water at room temperature. After regular intervals, the gels were removed from water and wiped with tissue paper to remove excess water from the surface of the gel. Then the change in weight was recorded. The process was repeated until no further change in weight was monitored. The final weight was used in the following equation to determine the weight swelling ratio of the gels. Swelling ratio (%) was calculated by the following formula,

$$\frac{Wt_{\text{swelled gel}}(g) - Wt_{\text{initial gel}}(g)}{Wt_{\text{initial gel}}(g)} \times 100 \qquad \text{(Equation 1)}$$

Swelling ratio measurement of the hydrogels at different pH: The hydrogels were prepared as described above using different concentrations of PAH {0.6 gm (9.4 μmol), 0.9 gm (14 μmol) and 1.2 gm (19 μmol)} and fixed concentration of cross linkers, i.e. DTDA (0.4 gm, 2.2 mmol, 0.7 mol/L), DEM (0.4 gm, 2.2 mmol, 0.7 mol/L), AA (0.2 gm, 2.2 mmol, 0.7 mol/L) or PEGDA (0.6 gm, 2.2 mmol, 0.7 mol/L). The resulting hydrogels were washed with water and weighed preceding to the swelling ratio studies. The gels were transferred to the beakers containing different pH buffer solutions. The buffer compositions were as follows; pH 2 (50 mL of 200 mmol/L KCl + 13 mL of 200 mmol/L HCl), pH 4 (100mL of 100 mmol/L KHP + 0.2 mL of 100 mmol/L HCl), pH 6 (100 mL of 100 mmol/L KH_2PO_4 +

11.2 mL of 100 mmol/L NaOH), pH 8 (100 mL of 100 mmol/L KH_2PO_4 + 93.4 mL of 100 mmol/L NaOH), pH 10 (100 mL of 50 mmol/L $NaHCO_3$ + 21.4 mL of 100 mmol/L NaOH). After regular intervals, the gels were removed from water and wiped with tissue paper to remove excess water from the surface of the gel. Then the change in weight was recorded. The process was repeated until no further change in weight was monitored. Swelling ratio (%) was calculated using Equation 1.

Encapsulation and release of dye: A typical procedure is described as follows; Rhodamine B (1.0 mg, 2.1 μmol) was added to the solution containing PAH (0.6 gm, 9.4 μmol) and DTDA {0.4 gm (2.2 mmol, 0.7 mol/L), 0.7 gm (3.9 mmol, 1.3 mol/L) or 1.0 gm (5.6 mmol, 1.9 mol/L)}. The mixture was kept undisturbed at room temperature for 30 min to release trapped air bubbles. The mixture was then heated up to 70 °C for 11 h to form the gel. The un-encapsulated dye was removed by washing the synthesized hydrogel with water repeatedly. The % encapsulation of the dye was quantified by comparing the absorbance at 554 nm of the initial concentration of the dye to that of the washing solution (**Table S1**). The gel was then dipped into pH ≈ 5.0 solution and maintained at 37 °C. UV–Vis spectroscopic analysis of the aqueous solution was recorded after regular time intervals to determine the extent of release. The % release was calculated using the following expression;

$$\frac{\text{Absorbance}_{\text{aqueous media after time "t"}}}{\text{Absorbance}_{\text{1 mg dye in 10 mL media}}} \times 100 \qquad \text{(Equation 2)}$$

Cell lines and culture conditions: NIH/3T3 (mouse embryonic fibroblast) cells were considered to evaluate the cytoxicity assay. Cells were maintained and passaged in DMEM supplemented with 10% fetal bovine serum and 1% penicillin/streptomycin. The cells were grown in 75 cm^2 cell culture flask with the appropriate medium at 37 °C humidified incubator with 5% CO_2. For this study, cells were used before the passage number 4.

Effect of hydrogel properties on cell viability (proliferation): After having 70% of confluence, the cells were trypsinized with 0.25% trypsin-0.1% EDTA solution and were counted using automated cell counter. Approximately, $1x10^6$ cells/mL were encapsulated in the hydrogels (PAH-DTDA, PAH-DEM, PAH-AA and PAH-PEGDA) synthesized at 37 °C using [PAH] = 0.2 gm/mL and [cross-linker] = 0.4 mol/L, in 1:1 ratio of media containing cell and hydrogel. Before hydrogel synthesis, the precursor polymer and cross-linkers were exposed to UV light for 45 min for sterilization purposes. Then 30 µL/well of each cell encapsulated hydrogels was placed on the 96 well plates. After 6 hours, about 70 µL of DMEM complete media was added to the above mixture.

MTT assay: On the next day (24 h post hydrogel formation), the plates were treated with 10 µL of MTT solution (5 mg/mL) at a final concentration of 0.5 mg/mL and kept in the 37 °C incubator. After 4 h, the remaining media was completely removed. The formazan crystals formed were dissolved in MTT detergent (10% SDS in 0.01 N HCl) and absorbance of the coloured solution was quantified at O.D. 570 nm.

EB/AO staining assay: Live/Dead assay was performed using EB/AO for the detection of live, apoptotic and necrotic cells.[29] A dye-mix of AO/EB (100 µg/mL AO and 100 µg/mL of EB) in phosphate buffered saline (PBS), pH 7.4 (137.0 mmol/L NaCl + 2.7 mmol/L KCl + 10.1 mmol/L Na_2HPO_4 + 1.8 mmol/L KH_2PO_4) was prepared and 8 µL of the dye-mix was added per well of the 96-well plate. The photographs were taken using DM IL LED inverted microscope. AO permeates all the cells and makes nuclei to appear green. EB dominates over AO and are taken up by the cells which have lost cytoplasmic membrane integrity and stains the nuclei red. Thus live cells have a normal green nucleus; early apoptotic cells have bright green nucleus with condensed or fragmented chromatin; late apoptotic cells display condensed and fragmented orange chromatin; cells those have died from direct necrosis have a structurally normal orange nucleus.

Results and discussion

Commonly used injectable materials for tissue engineering applications are peptide amphiphiles.[30,31] However, scalability is a major issue in these class of materials. In this article, we report convenient synthesis of a new set of cost effective injectable hydrogels using PAH as the precursor through hydrazide based click reactions. PAH was synthesized from PMA using a procedure reported elsewhere.[23] Due to the swift reactivity of carbonyl hydrazide functionality with a range of functional groups such as carboxylates, carboxylic acids and acrylates, a series of hydrogels were prepared from PAH using DTDA, AA, DEM and PEGDA as the cross-linkers (**Scheme 1**).[32,33] The aqueous solutions of PAH and cross-linkers in different molar proportions were kept either at room temperature or heated up to 70 °C to prepare the hydrogels. When DEM or PEGDA was used as the cross-linker, chemical cross-linking was primarily responsible for gelation, whereas in case of DTDA, a combination of chemical and reversible physical cross-linking determined the degree of cross-linking (**Scheme 1**). The nucleophilic substitution of carboxylate groups with $–CONHNH_2$ formed the chemical cross-linking and the hydrogen bonding between –S– and $–NH_2$ accounted for the physical cross-linking in the system. The PAH-AA hydrogels were synthesized through a dual cross-linking procedure. Michael type addition of $–CONHNH_2$ unit with acrylate functionality and electrostatic interaction between $–COO^-$ and $–CONHNH_3^+$ ions served as chemical and physical cross-link points, respectively (**Scheme 1**).

FT-IR spectra of the gels displayed characteristic bands suggesting successful cross-linking of the PAH with the linking agents (**Figure 1**). In case of PAH and DTDA based hydrogels, the band at 1730 cm^{-1} for the $–C=O_{str}$ of carboxylates disappeared and a new band at 1643 cm^{-1} accountable to the $–C=O_{str}$ of –***CO***NHNHCO- appeared suggesting quantitative cross-linking (**Figure 1A**). When DEM was used as the cross-linker, a similar shift in carbonyl frequency from 1731 cm^{-1} to 1605 cm^{-1} was noticed (**Figure 1B**). Characteristic

bands at 1635 and 1700 cm^{-1} owing to the –C=C– and –COOH groups respectively of AA disappeared and two new bands at 1653 and 1551 cm^{-1} accountable to the carboxylate and –***CO***NHNH– functionalities appeared in case of AA based gels as expected (**Figure 1C)**.

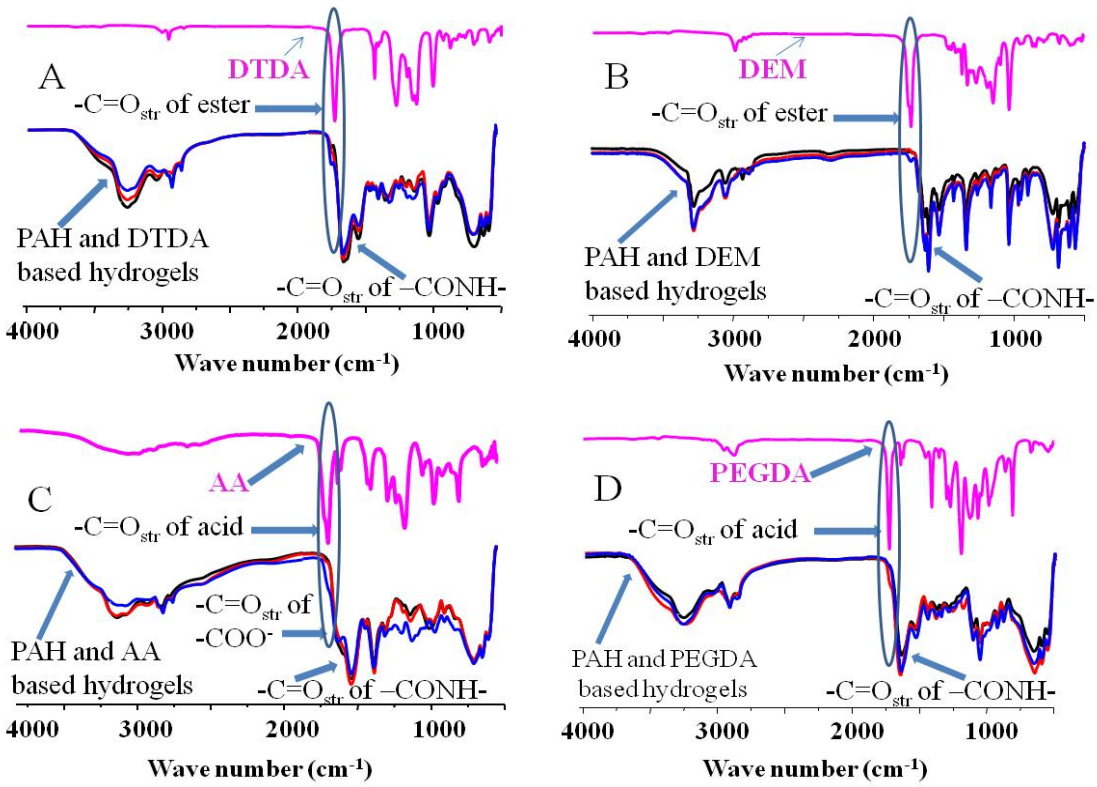

Figure 1: ATR FT-IR spectra of the cross-linkers and dehydrated (A) PAH-DTDA, (B) PAH-DEM, (C) PAH-AA and (D) PAH-PEGDA hydrogel thin films synthesized using 1.9 (——), 1.3 (——) and 0.7 (——) mol/L of cross-linkers in case of DTDA, DEM and AA and 0.7 (——), 0.4 (——) and 0.2 (——) mol/L in case of PEGDA.

Similarly, in case of PEGDA based gels, the disappearance of band at 1637 cm^{-1} accountable to the –C=C– of PEGDA suggested quantitative chemical cross-linking (**Figure 1D**). The [PAH]/[cross-linker] ratio was changed to synthesize a series of hydrogels with

different degrees of cross-linking. All the gels were transparent and defect free as shown in **Figure S1** (**Supporting Information**).

The effect of cross-linker concentration and weight% of PAH on gelation time is summarized in **Figure 2**. In case of PAH-DTDA, the gelation time decreased sharply on increasing the DTDA concentration (**Figure 2A**). However, a less pronounced effect on the gelation time was witnessed when DEM was used as the cross-linker (**Figure 2B**). For example, on increasing the DTDA concentration from 0.7 to 1.3 mol/L, the gelation time decreased by 50%, whereas similar variation in DEM concentration resulted in ~10% decrease in gelation time (**Figure 2B**). The above data suggested that DTDA may be having additional interactions with PAH apart from chemical cross-linking. One possible reason could be the hydrogen bond formation between the –S– moieties present in the DTDA with the –N–H of the $–CONHNH_2$ of PAH providing additional physical cross-linking to the system (**Scheme 1**). Thioethers were known to form hydrogen bonding with –O-H and –N-H groups readily.[34,35] To further support the above hypothesis, tensile analysis of the dehydrated strips of PAH-DTDA and PAH-DEM hydrogels were conducted. Higher ultimate tensile strength (UTS) = 4.9 MPa and lower elongation at break = 4.5% of the PAH-DTDA compared to that of the PAH-DEM (UTS = 1.6 MPa, elongation at break = 69.6%) supported the above hypothesis (**Table 1**). Higher Young's modulus (58.6 MPa) value of PAH-DTDA compared to that of the PAH-DEM (2.5 MPa) also suggested higher degree of entanglement. The gels synthesized using AA as the cross-linker exhibited lower gelation time compared to the other systems (**Figure 2**). This could be due to the involvement of $–NH_3^+$ and $–COO^-$ ion pair interaction in gel formation. The gelation time strongly decreased from 6 to 1 h with increase in AA concentration from 0.7 to 1.9 mol/L (**Figure 2C**). When PEGDA was used as the cross-linker only a moderate effect of cross-linker amount on the gelation time was

observed (**Figure 2D**). An increase in concentration from 0.2 to 0.7 mol/L of PEGDA resulted in ~35% decrease of the gelation time.

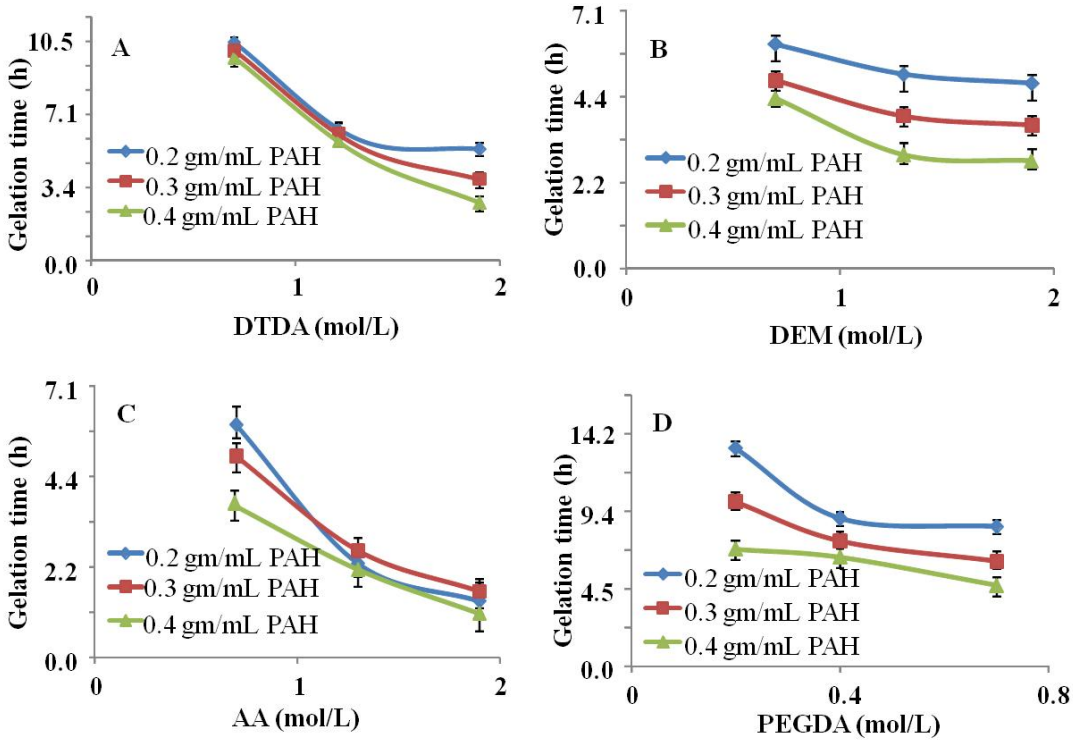

Figure 2. Effect of PAH and (A) DTDA, (B) DEM, (C) AA and (D) PEGDA concentration on the gelation time

Concentration of PAH had little effect on the gelation time in case of DTDA and AA based systems. However, when DEM and PEGDA were used as the cross-linkers, the gelation time somewhat decreased with increase in concentration of the solution. The data suggested, in case of samples where the gel formation was governed by chemical cross-linking only, the gelation time was moderately dependent on the concentration of PAH. The gelation times of the samples synthesized through dual cross-linking procedure was independent of PAH concentration. The above could be attributed to the large difference in

the rate of formation of physical and chemical cross-links. The rate of chemical reactions such as nucleophilic substitution of esters and Michael addition of double bonds depended on the concentration of reactants, whereas the effect of concentration on the rate of Zwitterionic interaction and hydrogen bond formation was negligible.

Table 1: Tensile data of dehydrated PAH-DTDA and PAH-DEM strips

Sample Code*	Tensile Strength (MPa)	Elongation at Break (%)	Young's Modulus (MPa)
PAH-DTDA	4.9 ± 0.9	4.5 ± 1.2	58.6 ± 7.1
PAH-DEM	1.6 ± 0.3	69.6 ± 5.0	2.5 ± 0.4

*the gels were prepared using 3.4 mol/L of the cross-linkers and 0.6 gm/mL of PAH in both the cases

Swelling ratio measurements

The swelling ratios of the hydrogels possessing different degrees of cross-linking were summarized in **Figure S2 (Supporting Information)**. In general, the swelling ratio was inversely proportional to the degree of cross-linking of the gels. The gels with higher degree of cross-linking were resistant to swelling due to higher degree of entanglement and rigidity. The swelling ratio of DTDA based gels was observed in the range of 20–350% depending on the [PAH]/[DTDA] ratio (**Supporting Information, Figure S2A**). Similarly, the swelling ratio of PAH-DEM hydrogels was observed in between 220 and 390% (**Supporting Information, Figure S2B**). The swelling ratios of AA and PEGDA based gels were in the range of 120–350% and 140–500% respectively under neutral pH and room temperature conditions. The moderately higher swelling ratio of PEGDA based gels compared to those of the other systems could be attributed to the hydrophilicity of PEG unit and longer distance between cross-link points in the gels (**Supporting Information, Figure S2D**). The swelling ratios of most of the compositions increased with increase in [PAH] (**Figure S2**). With

decrease in [cross-linker]/[PAH] ratio, the degree of cross-linking was expected to decrease. This may have decreased the rigidity and increased the swelling ratio of the system.

Figure S3 summarizes the effect of pH on the swelling ratios different hydrogels at room temperature. For this particular study, all the gels were synthesized using a fixed concentration of cross-linker and variable concentrations of PAH. As observed before, the swelling ratio decreased with increase in degree of cross-linking in all the cases. Under strongly acidic (pH = 2.0) conditions, significant syneresis occurred and minimum swelling was observed for all the samples (**Supporting Information, Figure S3).**The swelling ratios increased up to 200–300% on increasing the pH to 4.0. In the range of pH 4.0–8.0, the swelling ratio was comparable. For AA and PEGDA based systems, the swelling ratio reached maximum value under strongly basic conditions (pH 10.0), whereas for DTDA and DEM based systems, the swelling ratios were similar in the pH range of 4.0–10.0 (**Supporting Information, Figure S3).** The overall swelling ratios of the gels were in the range of 200–700% under basic pH conditions, whereas under neutral conditions, the swelling was limited to 50–500% suggesting the gels possess adequate pH responsiveness (**Supporting Information, Figure S2 and S3**).

Figure S4 summarizes the effect of both pH and temperature simultaneously on the swelling ratio of the gels prepared using 0.3 gm/mL PAH solution and 0.7 mol/L of the cross-linkers. With the increase in temperature, the swelling ratio of the hydrogels strongly decreased at pH = 2.0 suggesting severe syneresis. This could be due to the facile protonation of N-substituted and unsubstituted $–CONHNH_2$ moieties present in the gels to $–CONHNH_3^+$ and $–CONHNH_2^+–$ ions. As a result of which the extent of hydrogen bonding with the water molecules significantly decreased thereby decreasing the water-bearing capacity. On increasing the pH of the system to 4.0, the swelling ratio increased up to 400–700%. Maximum increase was noticed in case of DTDA and AA based hydrogels. The inherent

physical cross-links present in the above two systems increased the pH and temperature responsiveness of the systems and therefore any change in pH conditions of the medium resulted in large variation of swelling ratio. On increasing the pH from 4.0 to 6.0, the swelling ratio of PAH-DTDA decreased by ~100%. However, the swelling ratio was retrieved on further increasing the pH to 10.0 (**Supporting Information, Figure S4A**). In case of PAH-DEM, no significant change in swelling ratio was observed in the pH range of 6.0 to 10.0, whereas PAH-AA based systems exhibited a gradual increase in swelling ratio with increase in the pH from 6.0 to 10.0 (**Supporting Information, Figure S4B and C**). PAH-PEGDA samples showed a sharp increase in swelling ratio with increase in pH from 6.0 to 8.0 (**Supporting Information, Figure S4D**). The overall study suggested that, by changing the pH condition of the medium, the swelling ratio of the hydrogels may be controlled over a large range. However, in the pH range of 4.0 to 10.0, no notable effect of temperature on swelling ratio was observed in case all the gels.

Rheological behavior of gels

The hydrogels possessed chemical cross-links due to the reaction of carboxylate and acrylate functionalities of the cross-linkers with the carbonyl hydrazide pendant group of the PAH, whereas the –S---H–N– hydrogen bonding and Zwitterionic interactions accounted for the physical cross-links present in the system (**Supporting Information, Figure S5**).

To investigate the viscoelastic properties of the hydrogels, oscillatory rheological measurements were carried out at room temperature. **Figure 3** displays the storage (G′) and loss (G″) modulus of all the gels at different angular frequencies (ω). In all the cases, G′ was greater than G″ suggesting formation of rigid and stable chemically/physically cross-linked hydrogels. The G′ of the samples synthesized using 0.7 mol/L of the cross-linker was observed to be maximum in all the cases (**Figure 3**). However, the value significantly

decreased when the cross-linker concentration was increased to 1.9 mol/L. Interestingly, the G′ value of the sample synthesized using 0.7 mol/L was comparable to that of the gel synthesized using 1.3 mol/L of cross-linker (**Figure 3A, B and C**). Therefore, the mechanical properties were not only dependent on the chemical cross-links but also on various forms of physical cross-links present in the samples (**Supporting Information, Figure S5**).

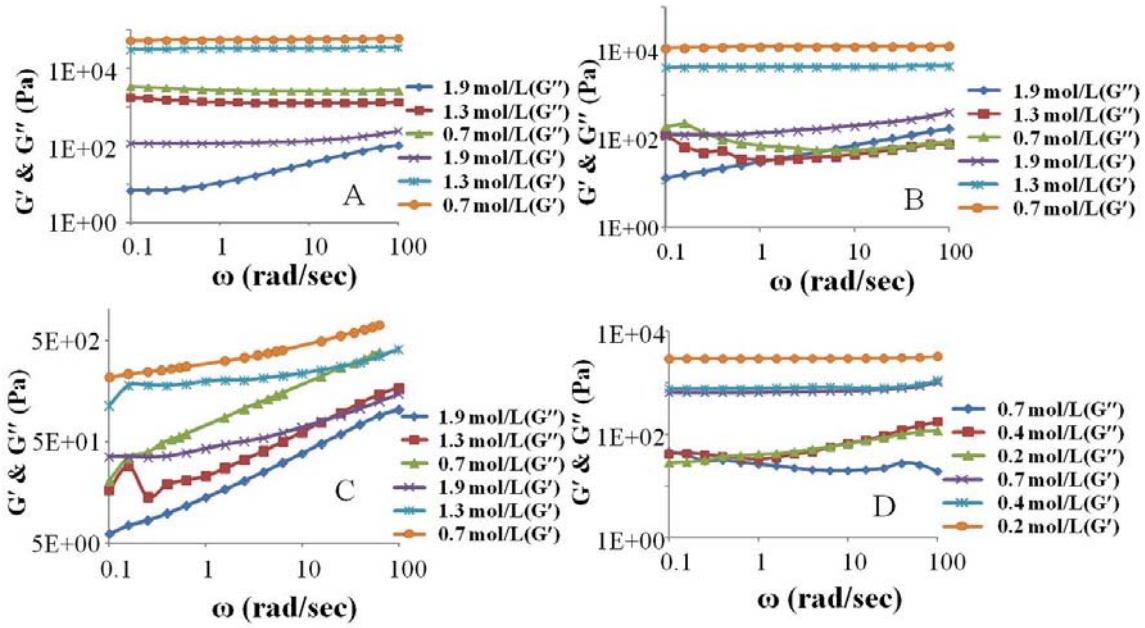

Figure 3: Oscillatory storage and loss modulus data of hydrogels prepared using (A) DTDA, (B) DEM, (C) AA and (D) PEGDA as the cross-linker.

The hydrogels synthesized using [DTDA] = 0.7 and 1.3 mol/L exhibited G′ in the range of 10^4 Pa. The linear regime was maintained over the entire frequency range. However, the G′ value significantly decreased by around two orders of magnitude on further increasing the cross-linker concentration to 1.9 mol/L and exhibited slight positive dependence on ω in the range of 1–100 rad/sec suggesting weak gelation behavior and brittleness of the samples resulting from excessive degree of cross-linking (**Figure 3A**). Similar phenomenon for

chemically cross-linked hydrogels has been reported in literature.[36] Though a similar trend in rheological behavior for PAH-DEM hydrogels to that of the PAH-DTDA based gels was observed, the G′ value for a particular concentration (0.7 or 1.3 mol/L) of cross-linker was higher in case of the later (**Figure 3B**). This could be attributed to the presence of physical along with chemical cross-links in the system (**Supporting Information, Figure S5**). The DTDA based hydrogel exhibited higher shear stress (3.5 kPa at 100% strain) and shear modulus (τ, 5.0 kPa) compared to the DEM based gels (Shear stress at 100% strain = 1.1 kPa, τ = 1.2 kPa) further supporting the above claim (**Supporting Information, Figure S6**). The G″ value decreased by one and two orders of magnitude compared to the G′ in case of DTDA and DEM based gels respectively (**Figure 3A and B**). The larger difference between G′ and G″ in case of the later suggested that the mechanical properties are driven by chemical cross-linking, whereas in case of the former some degree of physical cross-linking may be involved in determining the modulus. The tensile analysis of the dehydrated films well supported the rheology data (**Table 1**).

As anticipated, the G′ and G″ data of the AA based gels showed strong dependence to ω and the difference between the two decreased in higher ω region due to the involvement of weak physical cross-linking in gel formation unlike other gel systems (**Figure 3C**). The modulus values were also substantially lower than those of the DTDA and DEM based samples possessing same molar amount of cross-linkers. Maximum value for G′ was recorded for the sample prepared using [AA] = 0.7 mol/L and further increase in AA concentration resulted in gels with lower modulus (**Figure 3C**). Interestingly, the τ value (5.2 kPa) of the AA based hydrogel was comparable to that of the PAH-DTDA (5.0 kPa) and significantly higher than that of the PAH-DEM hydrogels (1.2 kPa) (**Supporting Information, Figure S6**). This could be due to the stress mediated reversibility of the Zwitterion interaction that

dissipated energy through cleavage and reformation of the bond as reported in case of other physically cross-linked systems.[37,38]

The G′ value of the gel synthesized using [PEGDA] = 0.7 mol/L was similar to that of the DEM based sample and the corresponding G″ value was lower by more than two order of magnitude compared to G′ (**Figure 3D**). The above data suggested, the mechanical properties were driven by mainly chemical cross-linking. However, the synthesis of gels with [PEGDA] ≥ 1.3 mol/L was not possible due to instant formation of non-uniform gels in aqueous medium. Therefore, samples were prepared with [PEGDA] = 0.4 and 0.2 mol/L and the mechanical properties were compared. The G′≈ 1000 Pa of the above two samples were similar and somewhat lower than that of the sample synthesized using [PEGDA] = 0.7 mol/L (**Figure 3D**). The above analysis suggested samples possessing 0.7 mol/L or less concentration of the cross-linker were stable with adequate mechanical properties and therefore were suitable for further analysis.

Injectability of the hydrogels

For adequate injectability, the gels were expected to possess yield stress, i.e. became liquid-like under applied stress and the viscosities were required to be low enough for smooth passage of the gel through injection needle. The viscoelastic response of the gels synthesized using 0.7 mol/L or less of the cross-linker was studied under variable strain to determine the yield behavior. The linear regime continued up to ~10% strain in all the cases as shown in **Figure 4**. The G′ of the gels synthesized using DTDA, AA or PEGDA as the cross-linker gradually decreased and the corresponding G″ increased on increasing the strain beyond 30% suggesting yielding of the samples. However, in case of DEM based samples the yielding behavior was not observed till 100% strain (**Figure 4**). The yield stresses of the gels were

observed in the range of 10–30% nominal strain suggesting the gels may be easily injected through a narrow path (**Figure 4**).

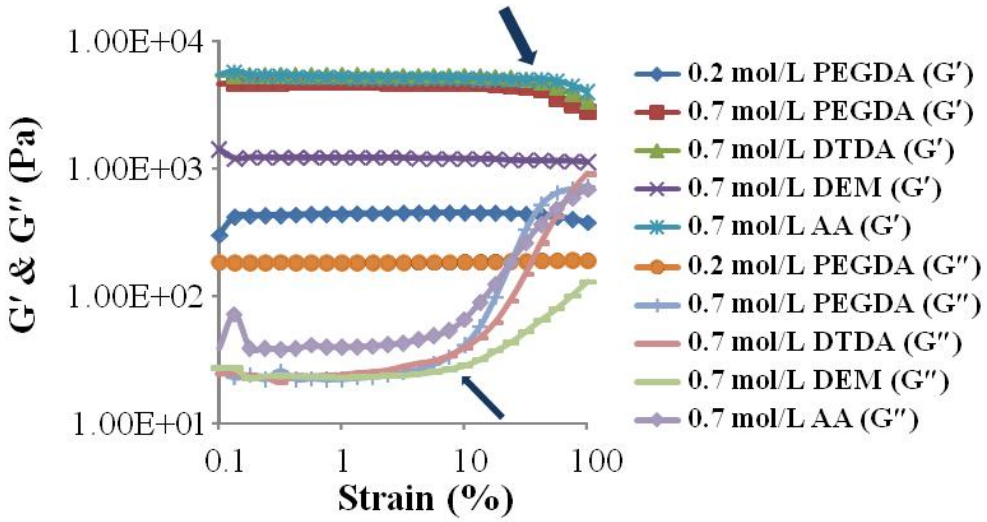

Figure 4: The strain sweep data of the hydrogels synthesized using 0.3 gm/mL PAH and cross-linkers at 10 rad/sec angular frequency

The shear thinning behavior of the hydrogels was studied further to verify the ease of injectability of the gels. The viscosity of the gels decreased by at least two orders of magnitude upon increasing the shear rate from ~1 to 1000 sec^{-1} displaying adequate shear thinning behavior (**Figure 5**). Shear thinning was also witnessed in case of the viscosity data obtained from frequency sweep measurements (**Supporting Information, Figure S7**). However, the viscosity data showed significant deviation from the Cox-Merz rule as the values were different from those of the frequency sweep data in most cases suggesting the samples were undergoing structural transformation under shear (**Table 2**). Similar phenomenon has already been reported in literature for urea based injectable hydrogels.[39]

Table 2: Comparison of viscosity data obtained from shear and frequency sweep experiments of PAH based hydrogels synthesized using different concentration of cross-linker.

Composition	Shear sweep		Frequency sweep	
-	Shear Rate	Viscosity	Angular Frequency	Viscosity
PAH(0.1 gm/mL)-PEGDA(0.2 mol/L)	63.4	0.9	63.1	1.7
PAH(0.2 gm/mL)-PEGDA(0.2 mol/L)	63.7	3.6	63.1	3.8
PAH(0.3 gm/mL)-PEGDA(0.2 mol/L)	63.5	32.7	63.1	14
PAH(0.3 gm/mL)-PEGDA(0.7 mol/L)	63.5	4.9	63.1	50.4
PAH(0.2 gm/mL)-DTDA(0.4 mol/L)	63.1	3.4	63.1	4.6
PAH(0.3 gm/mL)-DTDA(0.7 mol/L)	63.5	8.8	63.1	930
PAH(0.2 gm/mL)-AA (0.4 mol/L)	63.5	1.7	63.1	3.8
PAH(0.3 gm/mL)-AA (0.7 mol/L)	63.5	2.7	63.0	13

As can be seen in **Figure 5A and B**, the samples possessing physical cross-linking, i.e. PAH-AA and PAH-DTDA exhibited quantitative recovery of the viscosity. However, in case of the chemically cross-linked gels, the recovery was average and only up to 4–30% of the original viscosity was retrieved during the recovery scan of PAH-PEGDA samples (**Figure 5C, D and E**). The efficient recovery of viscosity in case of dual cross-linked gels could be attributed to the rapid reformation of physical cross-links on release of stress, which was not possible in chemically cross-linked system. The samples synthesized using higher concentration of cross-linkers (0.7 mol/L or higher) though exhibited substantial shear thinning behavior, the viscosity recovery was poor and therefore were not studied further (**Supporting Information, Figure S8).**

PAH-PEGDA hydrogels were used to study the effect of degree of cross-linking on injectability. As expected, on increasing the concentration of PAH from 0.1 to 0.3 gm/mL, the initial viscosity increased from 50 Pa.sec to 830 Pa.sec. The samples possessing lower degree of cross-linking exhibited marginally higher recovery compared to the samples with higher degree of cross-linking (**Figure 5C, D and E**).

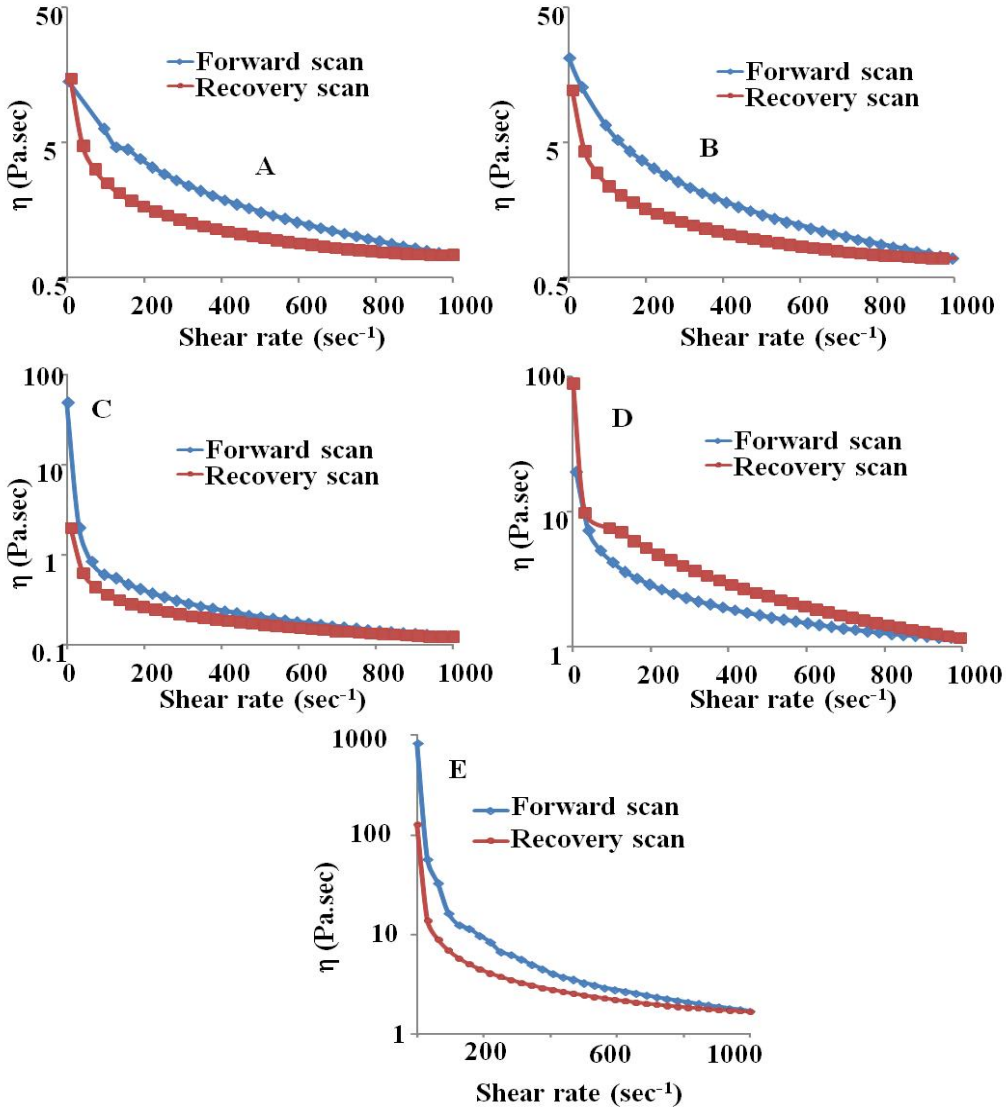

Figure 5: Reversible viscosity profile with respect to shear rate of the gels synthesized using (A) PAH (0.2 gm/mL) and AA (0.4 mol/L), (B) PAH (0.2 gm/mL) and DTDA (0.4 mol/L), (C) PAH (0.1gm/mL) and PEGDA (0.2 mol/L), (D) PAH (0.2 gm/mL) and PEGDA (0.2 mol/L) and (E) PAH (0.3 gm/mL) and PEGDA (0.2 mol/L).

For example, sample synthesized using [PAH] = 0.1 gm/mL showed 4% recovery of the viscosity during the recovery scan, whereas the sample having 0.2 gm/mL of PAH recovered up to 22% of the initial viscosity. However, attempts to improve the recovery

further by increasing the PAH concentration to 0.3 gm/mL was unsuccessful, as the viscosity of the resulting sample recovered only up to ~20% (**Figure 5E**). However, noticeable syneresis was observed during recovery scans of all the samples. Simple demonstrations of the injectability were shown in the **Figures 6** and **S9 (Supporting Information)** for the PAH-AA hydrogel, where the gel became solid like after ejection from the needle.

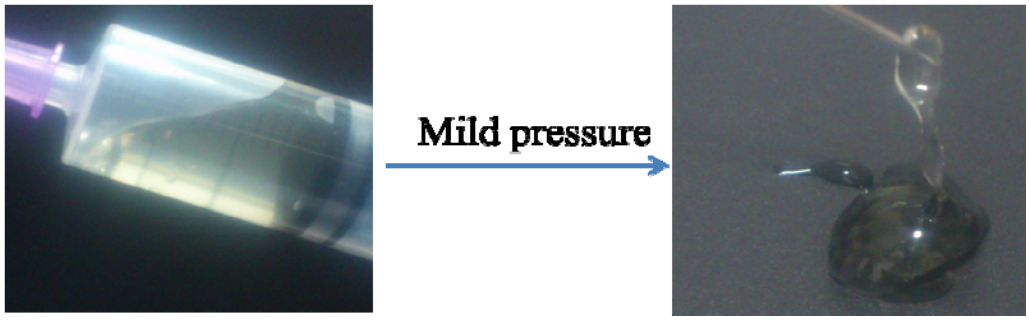

Figure 6: Photographs depicting the injectability of the PAH (0.2 gm/mL)-AA (0.4 mol/L) hydrogel.

Stability of hydrogels

As anticipated, the water retention capacity was related to the degree of cross-linking of the hydrogels (**Supporting Information, Figure S10)**. All the hydrogels prepared using 0.7 or 1.3 mol/L of the DTDA or DEM showed minimal loss (2–28%) in water content up to 40 days suggesting adequate gel stability. However, the hydrogels synthesized using 1.9 mol/L of the cross-linker exhibited noticeable syneresis and released up to ~45% water during the period of 40 days (**Supporting Information, Figure S10)**. Slow collapse may be attributed to slow physical bond formation as the restricted self-diffusion of the polymer chains occurred within the gel. To study the potential influence of hydrolysis on water retention capacity, the extent of hydrolysis of the chemical cross-links (-CONHNHCO-) was determined by FT-IR spectroscopic analysis. A small (~6.5%) increase in transmittance of –

$C=O_{str}$ (–CONHNHCO-) after 38 days suggested that minor amount of hydrolysis may have occurred during the period (**Supporting Information, Figure S11**). In case of PAH-AA hydrogels, only the samples prepared using 0.7 mol/L or less amount of AA showed adequate stability up to 40 days by releasing up to 15% of water during the period. The gels prepared using 1.3 and 1.9 mol/L of AA lost significant amount of water (44–48%) over 40 days (**Supporting Information, Figure S10)**. The above trend was expected since in this particular case, the gelation occurred through weak physical cross-linking procedure. The gels based on PEGDA showed exceptional water retention capacity for all concentrations (0.2–0.7 mol/L) of the cross-linker as negligible weight loss was observed after 40 days due to the presence of hydrophilic PEG moiety. From FT-IR spectroscopic analysis, the extent of hydrolysis of PAH-PEGDA (0.7 mol/L) hydrogel was calculated to be ~1% (**Supporting Information, Figure S12)**. The above hydrolysis data of the hydrogels suggested that the influence of hydrolysis on water retention capacity may be negligible during the study period. Overall, samples possessing cross-linker concentrations up to 0.7 mol/L exhibited minimal change in water retention capacities up to 40 days at room temperature.

Controlled release of dye

In past, pH responsiveness of various hydrogels has been utilized as an effective tool to release encapsulated entities in a controlled manner.[40,41] Similarly, encapsulation and release behavior of the PAH based hydrogels was studied using Rhodamine B as the dye. A fixed amount of dye was added to the precursor solution for in-situ encapsulation. The % encapsulation (96.6–99%) was determined by comparing the absorbance of initial concentration of the dye to that of the washing solution (**Table S1**). The dye release at 37 °C in pH = 5.0 solution was monitored after regular time intervals by UV–Vis spectroscopic analysis. The release rate and amount depended on the type of cross-linker and degree of

cross-linking (**Figure 7**). In case of DTDA based hydrogels, the release increased with the increase in degree of cross-linking and a maximum release of ~56% of the original loading was witnessed after 120 h for the hydrogel prepared using 1.9 mol/L of DTDA. In PAH-DEM hydrogels, the overall release was limited to ~40%. The samples prepared using [DEM] = 0.7 and 1.3 mol/L showed higher dye release compared to that of the gel containing 1.9 mol/L of DEM. Since the extent of swelling was not significant (≤ 300%), increase in cross-linking hampered the release capacity of the gel. Higher release of the dye in case of PAH-DTDA compared to the PAH-DEM could be attributed to the enhanced pH responsiveness resulting from the inherent –S---H-N- hydrogen bonding interactions (**Supporting Information, Figure S5A**).

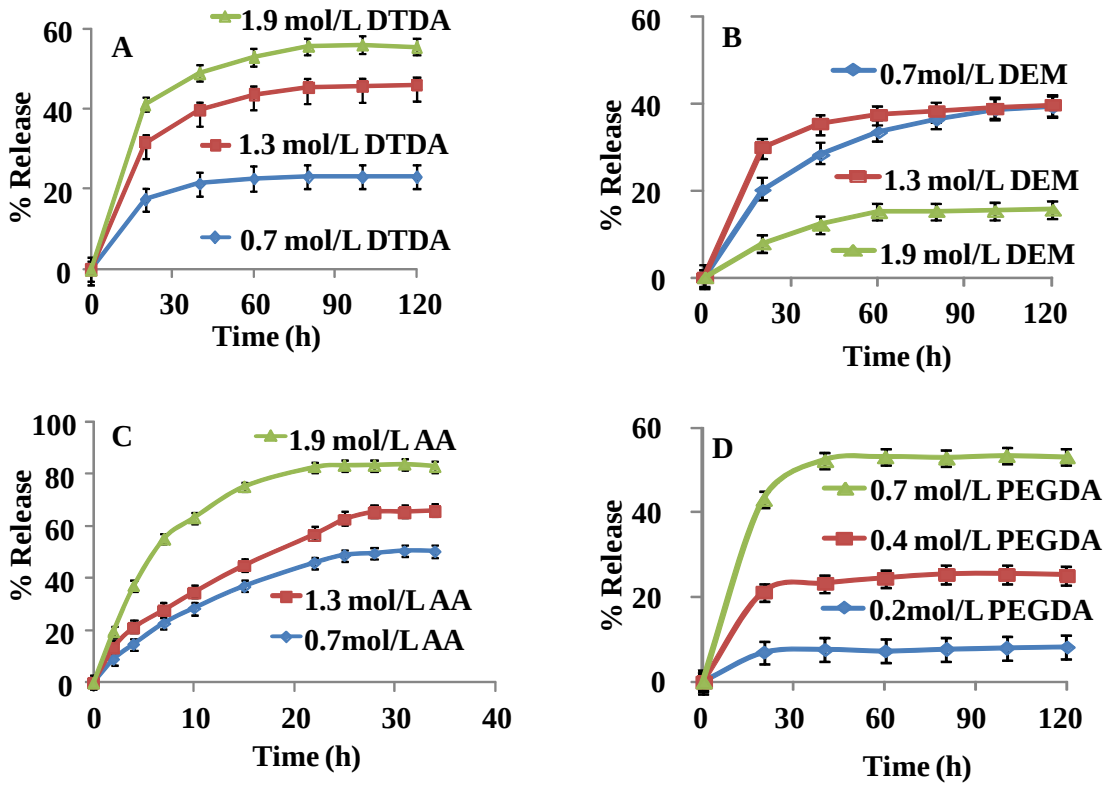

Figure 7: Controlled release profile of Rhodamine B from the hydrogels synthesized using 0.2 g/mL of PAH and (A) DTDA, (B) DEM, (C) AA or (D) PEGDA.

The release rate from PAH-AA hydrogels was comparatively faster than other three systems. Probably, the weak Zwitterionic interaction present in the system easily dissociated under weakly acidic (pH 5.0) conditions. Therefore, release up to 84% of the original loading was witnessed in a short period of less about 40 h (**Figure 7C**). In case of PAH-PEGDA gels, maximum release was noticed in case of the sample synthesized using 0.7 mol/L. Samples with [PEGDA] = 0.4 and 0.2 mol/L exhibited relatively poor release (10–25%) of the dye (**Figure 7D**).

Cytotoxicity analysis

The cytocompatibility studies were conducted in vitro on the hydrogels synthesized at 37 °C using 0.2 gm/mL of PAH and 0.4 mol/L of cross-linkers (**Figure 8 and 9**). The mouse embryonic fibroblasts (NIH3T3) were added to the solution of PAH and cross-linker prior to gelation for effective encapsulation. The cell viability of the NIH3T3 encapsulated gels were studied using live dead assay and MTT assay. As shown in **Figure 8,** more than 90% of the living cells were visualized in all four types of hydrogels.

In MTT assay, a similar cell viability profile could be observed (**Figure 9**). Especially, the hydrogel synthesized using PEGDA and AA exhibited excellent cytocompatibility compared to those of the DTDA, DEM. The level control cell in **Figure 9** indicates the viability reading of same density of cells plated on a multiwell plate. The enhanced cytocompatiblity of PEGDA based gels compared to others could be attributed to the presence of hydrophilic PEG segment in the cross-linker. The cytocompatibility of PEG based hydrogels are well documented in literature.[42,43] The overall cytocompatibility and injectability data indicated the samples are suitable materials for various biomedical applications.

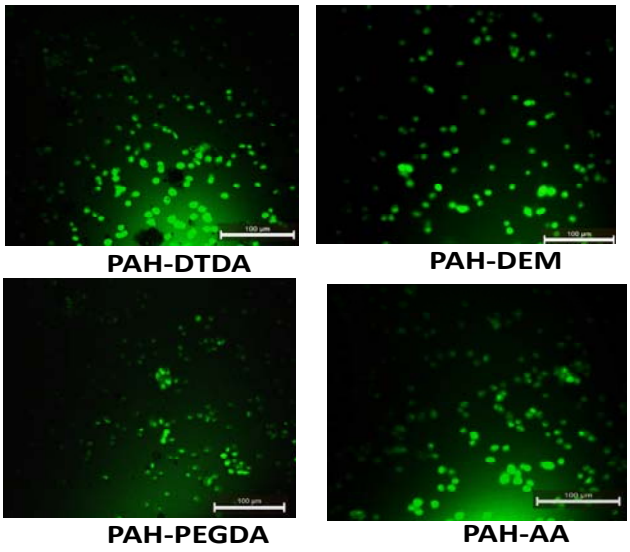

Figure 8: Mouse embryonic fibroblasts (NIH/3T3) were encapsulated in the indicated hydrogels in 96 well plates for 24 h after which a dye-mix of AO/EB (100 µg/mL AO and 100 µg/mL of EB in PBS pH 7.4) was prepared and 8 µL of the dye-mix was added per well of 96-well plate. Fluorescence microscopy was performed to analyze the live and dead cells.

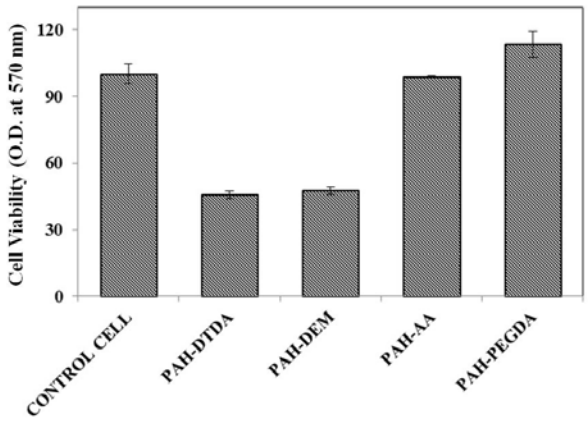

Figure 9: Mouse embryonic fibroblasts were encapsulated in indicated hydrogels in 96 well plates for 24h after which MTT solution was added at a final of 0.5 mg/mL and kept in the 37 °C incubator. After 4 hours the remaining media was completely removed and Formosan crystals formed were dissolved in MTT detergent and the absorbance of the colored solution was quantified at O.D. 570 nm. For SD, n=3

Conclusion

PAH based Hydrogels with tunable swelling ratio and mechanical properties can be synthesized using a range of cross-linkers employing hydrazide based click reactions. Though, four examples of cross-linkers are described in this report, the list is not limited to the above. The mechanical properties of the gels can be readily altered by controlling the degree of chemical and physical cross-linking in the samples. Substantial shear thinning and rapid recovery make these hydrogels suitable injectable materials at high storage modulus. The injectability may be optimized by varying the molar ratio of cross-linkers and concentration of PAH. Especially the samples synthesized through dual cross-linking procedure are more suitable for injectability application compared to the chemically cross-linked samples. The release of probe molecules by the hydrogels was efficient and may be further tuned by changing the linker as well as degree of cross-linking. The hydrogels possessed adequate cytocompatibility and therefore are potential candidates for various biomedical applications.

Acknowledgements

AK and SKS acknowledge CSIR-India for the Junior Research Fellowship. Department of Science & Technology (DST)-India (Grant: SERB/F/5311/2012-13) is acknowledged for providing partial financial assistance for the research. RD is a Department of Biotechnology-India Ramalingaswami Fellow.

Notes

The Authors declare no competing financial interest.

Corresponding Author

E Mail: uojha@rgipt.ac.in

Tel: 0535-270-4221, Fax: 0535-221-1888

Author Contributions

The article was written through the contribution of all the authors and all the authors have given approval to the final version of the manuscript.

† Department of Chemistry, Rajiv Gandhi Institute of Petroleum Technology Rae Bareli

‡ Institute of Life Science, Bhubaneswar, Odisha

Supporting Information Available

The photographs of hydrogels, swelling ratio of the hydrogels at fix temperature with different cross linkers or fix temperature with different concentration of PAH and fix concentration of cross linkers or different temperature with fix concentration of PAH and cross linkers, schematics showing the type of physical and chemical crosslinking units, shear stress versus strain plot, frequency versus complex viscosity plot, viscosity versus shear rate plot, photographs depicting the injectability, water retention capacities of PAH based hydrogels, percentage encapsulation of Rhodamine B in PAH based hydrogels and ATR FTIR spectra of the DTDA & PEGDA based hydrogels. This information is available free of charge via the Internet at http://pubs.rsc.org/.

References:

1) H. Qi, M. Ghodousi, Y. Du, C. Grun, H. Bae, P. Yin and A. Khademhosseini, *Nat. Commun.*, 2013, **4,** 3275–3283.

2) S. M. Mihaila, A. K. Gaharwar, R. L. Reis, A. P Marques, M. E. Gomes and A. Khademhosseini, *Adv. healthcare mater.*, 2013, **2,** 895–907.

3) W. M. Gramlich, I. L. Kim and J.A Burdick, *Biomaterials*, 2013, **34,** 9803–9811.

4) S. J. Kim, G. M. Spinks, S. Prosser, P. G Whitten, G. G. Wallace and S. I. Kim, *Nat. mater.*, 2006, **5,** 48–51.

5) J. Randall, M. A. B. Meador and S. C. Jana, *ACS Appl. Mater. Interfaces*, 2011, **3,** 613–626.

6) U. Gulyuz and O. Okay, *Soft Matter*, 2013, **9,** 10287–10293.

7) B. S. Tucker, and B. S. Sumerlin, *Polym. Chem.*, 2014, **5,** 1566–1572.

8) M. He, J. Li, S. Tan, R. Wang and Y. Zhang, *J. Am. Chem. Soc.*, 2013, **135,** 18718–18721.

9) X. Li, E. Katsanevakis, X. Liu, N. Zhang and X. Wen, *Prog. Polym. Sci.*, 2012, **37,** 1105–1129.

10) E. F. Banwell, E. S. Abelardo, D. J. Adams, M. A. Birchall, A. Corrigan, A. M. Donald, M. Kirkland, L. C. Serpell, M. F. Butler, and D. N. Woolfson, *Nat. Mater.*, 2009, **8,** 596–600.

11) A. P. Vogt and B. S. Sumerlin, *Soft Matter*, 2009, **5,** 2347–2351.

12) J. Wang, D. D. N. Sun, Y. Shin-ya and K. W. Leong, *Macromolecules*, 2004, **37,** 670–672.

13) Z. Lin, W. Gao, H. Hu, K. Ma, B. He, W. Dai, X. Wang, J. Wang, X. Zhang and Q. Zhang, *J. Controlled Release*, 2014, **174,** 161–170.

14) A. Baral, S. Roy, A. Dehsorkhi, I. W. Hamley, S. Mohapatra, S. Ghosh and A. Banerjee, *Langmuir*, 2014, **30,** 929–936.

15) O. Jeon and E. Alsberg, *Adv. Funct. Mater.*, 2013, **23,** 4765–4775.

16) S. A. Zawko, S. Suri, Q. Truong and C. E. Schmidt, *Acta Biomater.*, 2009, **5,** 14–22.

17) W.-C. Lin, W. Fan, A. Marcellan, D. Hourdet and C. Creton, *Macromolecules*, 2010, **43,** 2554–2563.

18) K. Haraguchi and T. Takehisa, *Adv. Mater.*, 2002, **14,** 1120–1124.

19) T. Potta, C. J. Chun and S.-C. Song, *Biomacromolecules*, 2010, **11,** 1741–1753.

20) T. Narita, K. Mayumi, G. Ducouret and P. Hebraund, *Macromolecules*, 2013, **46,** 4174–4183.

21) A. K. Ekenseair, K. W. M. Boere, S. N. Tzouanas, T. N. Vo and A. G. Mikos, *Biomacromolecules*, 2012, **13,** 2821−2830.

22) T. N. Vo, A. K. Ekenseair, F. K. Kasper and A. G. Mikos, *Biomacromolecules*, 2014, **15,** 132–142.

23) A. Kumar, R, R. Ujjwal, A. Mittal, A. Bansal and U. Ojha, *ACS Appl. Mater. Interfaces*, 2014, **6,** 1855–1865.

24) C. Lu, X. Wang, G. Wu, J. Wang, Y. Wang, H. Gao and J. Ma, *J. Biomed. Mater. Res., Part A*, 2014, **102,** 628–638.

25) M. Patenaude, S. Campbell, D. Kinio and T. Hoare, *Biomacromolecules*, 2014, **15,** 781–790.

26) T. Ito, Y. Yeo, C. B. Highley, E. Bellas and D. S. Kohane, *Biomaterials*, 2007, **28,** 3418–3426.

27) X. Z. Shu, Y. Liu, F. S. Palumbo, Y. Luo and G. D. Prestwich, *Biomaterials*, 2004, **25,** 1339–1348.

28) N. Agarwal, C.-H. Hung and M. Ravikanth, *Tetrahedron*, 2004, **60,** 10671–10680.

29) D. Ribble, N. B. Goldstein, D. A. Norris and Y.G. Shellman, *BMC Biotechnology*, 2005, **5,** 5−12.

30) H. D. Lu, M. B. Charati, I. L. Kim and J. A. Burdick, *Biomaterials*, 2012, **33,** 2145−2153.

31) E. L. Bakota, Y. Wang, F. R. Danesh and J. D. Hartgerink, *Biomacromolecules*, 2011, **12,** 1651−1657.

32) S. Binauld, W. Scarano and M. H. Stenzel, *Macromolecules*, 2012, **45,** 6989–6999.

33) J. R. Rasmussen, D. E. Bergbreiter and G. M. Whitesides, *J. Am. Chem. Soc*., 1977, **99,** 4746–4756.

34) H. S. Biswal and S. Wategaonkar, *J. Phys. Chem. A*, 2010, **114,** 5947–5957.

35) P. Du, X.-K. Jiang and Z.-T. Li, *Tetrahedron Lett.*, 2009, **50,** 320–324.

36) H. Shin, B. D. Olsen and A. Khademhosseini, *Biomaterials*, 2012, **33,** 3143–3152.

37) K. J. Henderson, T. C. Zhou, K. J. Otim and K. R. Shull, *Macromolecules*, 2010, **43,** 6193–6201.

38) J. Yang, F.-K. Shi, C. Gong and X.-M. Xie, *J. Colloid Interface Sci.*, 2012, **381,** 107–115.

39) G. M. Pawar, M. Koenigs, Z. Fahimi, M. Cox, I. K. Voets, H. M. Wyss and R. P. Sijbesma, Biomacromolecules, 2012, **13**, 3966–3976.

40) J. P. Schillemans, E. Verheyen, A. Barendregt, W. E. Hennink and C. F. V. Nostrum, *J. Controlled Release*, 2011, **150,** 266–271.

41) J. Wu and M. J. Sailor, *Adv. Funct. Mater*., 2009, **19,** 733–741.

42) K. B. Bjugstad, D. E. Redmond, K. J. Lampe, J. R. Sladek and M. J. Mahoney, *Cell Transplant*, 2008, **17,** 409–415.

43) L. Zhang, Y. Jeong, S. Zheng, S. I. Jang, H. Suh, D.H. Kang and I. Kim, *Polym. Chem.*, 2013, **4,** 1084–1094.